PHYSICAL REVIEW B **70**, 144207 (2004)

Application of renormalization and convolution methods to the Kubo-Greenwood formula in multidimensional Fibonacci systems

Vicenta Sánchez[1] and Chumin Wang[2]

[1]*Departamento de Física, Facultad de Ciencias, Universidad Nacional Autónoma de México (UNAM), Apartado Postal 70-542, 04510, México D.F., México*

[2]*Instituto de Investigaciones en Materiales, UNAM, Apartado Postal 70-360, 04510, México D.F., México*

(Received 10 March 2004; revised manuscript received 28 June 2004; published 29 October 2004)

Based on the Kubo formalism, electronic transport in macroscopic quasiperiodic systems is studied by means of an efficient renormalization method, and the convolution technique is used in the analysis of two- and three-dimensional lattices. For the bond problem, we found a transparent state located at a center of self-similarity and its ac conductivity is qualitatively different from that observed in mixing Fibonacci chains. The conductance spectra of multidimensional systems exhibit a quantized behavior when the electric field is applied along a periodically arranged atomic direction, and it becomes a devil's stair if the perpendicular subspace of the system is quasiperiodic. Furthermore, the dc conductance maintains a constant value for small imaginary parts (η) of the energy and decays when $\eta > \eta_c$, where η_c is proportional to the inverse of the system length. Finally, the spectrally averaged conductance shows a power-law decay as the system length grows, neither constant as in periodic systems nor exponential decays occurred in randomly disordered lattices, revealing the critical localization nature of the eigenstates in quasicrystals.

DOI: 10.1103/PhysRevB.70.144207 PACS number(s): 71.23.Ft, 72.15.−v, 05.10.Cc

I. INTRODUCTION

Since the discovery of quasicrystalline alloys in 1984, the electronic transport in quasiperiodic systems has been a controversial subject, because it is not expected to be ballistic as in periodic lattices neither diffusive as in randomly disordered ones.[1] These alloys possess an extremely low conductivity for their metallic constituents, and become more resistive when they are more perfect, which are believed to be a consequence of the quasiperiodicity of the system.[2] Their optical conductivity is also unusual, showing a linear frequency dependence and no Drude peaks.[3] Nowadays, there is a consensus that the eigenvalue spectrum produced by a quasiperiodic potential is singular continuous and the associated eigenfunctions are critical.[4] The relationship between this exotic localization of states and the anomalous transport phenomena is not fully understood.

In quasiperiodic systems, concepts like the reciprocal space become useless, and then the real-space renormalization technique seems to be the unique medium to investigate truly macroscopic lattices.[5–9] Recently, we have developed a novel renormalization method for the Kubo-Greenwood formula in mixing Fibonacci chains, finding scale invariances in the dc and ac conductivity spectra around the transparent state.[10] It is important to mention that this renormalization procedure is difficult to be extended to multidimensional systems, since for each generation only the interior sites of the lattice can be renormalized and all the border sites should be explicitly kept in order to calculate the Green's function of next generations, i.e., for a d-dimensional system, the number of border sites increases as a system of $d-1$ dimensions,[11] except $d=1$ where the number of border sites is always two. An alternative way to address the multidimensional quasiperiodic systems is through the convolution technique, when the Hamiltonian of the system is separable.[12] For instance, the decagonal quasicrystals can be visualized as a periodic stacking of quasiperiodic layers and their Hamiltonian can be expressed as a sum of the periodic and quasiperiodic parts within the nearest-neighbor tight-binding approximation. In this paper, we report an extension of the previously developed renormalization method to the bond problem and an analysis of the electronic conductance in two- and three-dimensional quasiperiodic systems by using the convolution technique.

This article is organized as follows: Sec. II defines the system and introduces the renormalization method. Its iterative formulas are given in Appendix A. In Sec. III, the dc and ac conductivity spectra of a Fibonacci chain with two kinds of bonds are analyzed in comparison with those of the mixing problem. In particular, their scaling behaviors are studied in detail. In Sec. IV, the electrical conductances of two- and three-dimensional quasiperiodic systems are investigated by means of the convolution method, which is carefully addressed in Appendix B. Quantized conductance spectra are obtained for periodic systems and these spectra become fractal ones when in the perpendicular direction to the applied electric field the atoms are quasiperiodically arranged. The spectral average of the conductance reveals a power-law decay as the system length grows. The effects of the imaginary part (η) of the energy on the Kubo conductivity is also analyzed. An analytical solution of this analysis for the periodic case is given in Appendix C. Finally, Sec. V summarizes the results and provides some conclusive remarks.

II. THE FIBONACCI CHAINS

There are various manners to build a Fibonacci chain, for example, by using two sorts of bonds (bond problem), two kinds of atoms (site problem) or a combination of both (mixing problem).[13] In this paper, we study the bond problem, in which two bond strengths, t_A and t_B, are organized following the Fibonacci sequence and the nature of the atoms are assumed to be the same, i.e., their self-energies $\alpha_j=0$. This problem has the advantage of being easily extendible to multidimensional quasiperiodic lattices, as shown in next sections. Let us define the first and the second generations of the Fibonacci sequence as $F_1=A$ and $F_2=BA$, respectively. The next generations are given by $F_n=F_{n-1}\oplus F_{n-2}$, containing $N(n)$ atoms for a chain of generation n. For instance, $F_5=BAABABAA$. For the sake of simplicity, a uniform bond length (a) is taken. Along the applied electric field all the systems considered in this paper are connected to two semi-infinite periodic leads with null self-energies, hopping integrals t and a lattice constant a, in order to resemble the measurement conditions. The effects of different boundary conditions on the electrical conductivity have been analyzed in Ref. 10.

In order to isolate the quasicrystalline effects on the physical properties of the system, we consider a simple s-band tight-binding Hamiltonian,

$$H=\sum_j \{t_{j,j+1}|j\rangle\langle j+1| + t_{j-1,j}|j\rangle\langle j-1|\}, \tag{1}$$

where $t_{j,k}$ is the hopping integral between nearest-neighbor sites j and k. The analysis of the electrical conductivity (σ) is carried out by using the Kubo-Greenwood formula,[14]

$$\sigma(\mu,\omega,T)=\lim_{\Omega\to\infty}\frac{2e^2\hbar}{\pi\Omega m^2}\int_{-\infty}^{\infty} dE\,\frac{f(E)-f(E+\hbar\omega)}{\hbar\omega}\times \mathrm{Tr}[p\,\mathrm{Im}\,G^{+}(E+\hbar\omega)p\,\mathrm{Im}\,G^{+}(E)], \tag{2}$$

where Ω is the volume of the system, $G^{+}(E)$ is the retarded one-particle Green's function, $f(E)=\{1+\exp[(E-\mu)/k_BT]\}^{-1}$ is the Fermi-Dirac distribution with Fermi energy μ and temperature T, and p is the projection of the momentum operator along the applied electric-field direction. The latter can be determined by using the relations $p=(im/\hbar)[H,x]$ and $x=\Sigma_j x_j|j\rangle\langle j|$, being x_j the coordinate of site j. Thus, in the Wannier representation it is

$$p=\frac{ima}{\hbar}\sum_j \{t_{j,j+1}|j\rangle\langle j+1| - t_{j-1,j}|j\rangle\langle j-1|\}. \tag{3}$$

As a limit case, let us consider an infinite periodic linear chain with a lattice constant a, null self-energies and hopping integrals t. The conductivity of its segment of N atoms at $T=0$ can be analytically calculated, as shown Eq. (C5),

$$\sigma(\mu,\omega,0)=\frac{8e^2t^2a}{\pi(N-1)\hbar^3\omega^2}\left[1-\left(\frac{\mu}{2t}\right)^2\right]\times\left\{1-\cos\left[(N-1)\frac{\hbar\omega/(2t)}{\sqrt{1-[\mu/(2t)]^2}}\right]\right\}, \tag{4}$$

where $|\mu|\leqslant 2|t|$ and the system length is $\Omega=(N-1)a$. In the limit of $\omega\to 0$, the dc conductivity is

$$\sigma_p=\sigma(\mu,0,0)=\frac{e^2a}{\pi\hbar}(N-1). \tag{5}$$

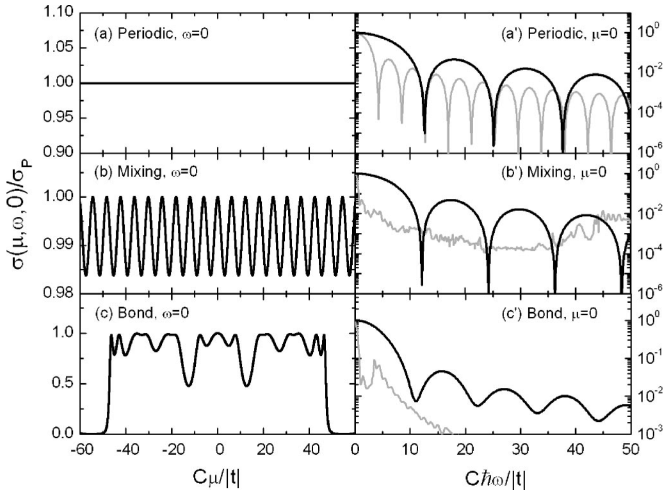

FIG. 1. The dc and ac Kubo conductivities $[\sigma(\mu,\omega,0)]$ for a periodic chain [(a) and (a′)] of generation $n=41$ with $\gamma=1.0$, a mixing Fibonacci chain [(b) and (b′)] with $n=41$ and $\gamma=t_{AA}/t_{AB}=0.88$, and a bond Fibonacci chain [(c) and (c′)] with $n=40$ and $\gamma=t_B/t_A=0.88$. All the systems are connected to two periodic linear leads of 10^{20} atoms and the imaginary part of the energy is $10^{-11}|t|$. The transparent state is located at $\mu=0$. The ac conduction behaviors for $\mu=-1.88348|t|$ in the three systems are illustrated by gray lines.

For the quasiperiodic case, we have developed an efficient renormalization method for the Kubo-Greenwood formula.[10] In particular, the recursion formulas corresponding to the bond problem are given in Appendix A, which allow us to evaluate the trace of Eq. (2) in an iterative way. For direct calculations of Eq. (2) the computing time grows as a third power of the system size, whereas using the renormalization procedure it grows linearly with the number of generation, i.e., grows logarithmically with the system size. For example, for a system with 988 atoms the direct-calculation time is 3932891 ms versus 27 ms if the renormalization method is used. It would be worth emphasizing that the results obtained by both methods are exactly the same. Therefore, in the rest of this paper we will use the renormalization method to evaluate the Kubo-Greenwood formula.

Figures 1(a)–1(c), respectively show the dc conductivities around $\mu=0$ of a periodic, a mixing $(n=41)$ and a bond $(n=40)$ Fibonacci chains. The on-site energies are null in these three systems and the hopping-parameter ratio (γ) are $\gamma=1$ for the periodic, $\gamma=t_{AA}/t_{AB}=0.88$ for the mixing and $\gamma=t_B/t_A=0.88$ for the bond problem, being $t_{AB}=t_A=t$. The imaginary part of the energy in the Green's function is $10^{-11}|t|$. Notice that in Fig. 1(c) $\sigma(0,0,0)=\sigma_P$, i.e., there is a transparent state in the bond problem. It can be analytically proved by means of the Landauer formula, in which the conductivity is proportional to the transmittance (τ) of the system.[15] In particular, for $\mu=0$ the transmittance is given by[13]

$$\tau(\mu=0)=\frac{4}{(m_{21}-m_{12})^2+(m_{11}+m_{22})^2}, \tag{6}$$

where m_{ij} are elements of the transfer matrix $[M(n)]$ defined by

$$M(n) = M_{N(n)}M_{N(n)-1}\cdots M_1, \tag{7}$$

being

$$M_i = \begin{pmatrix} \frac{\mu-\alpha_i}{t_{i,i+1}} & \frac{t_{i,i-1}}{t_{i,i+1}} \\ 1 & 0 \end{pmatrix}. \tag{8}$$

It has been shown that for mixing Fibonacci systems with $\alpha_A=\alpha_B=0$ there is a transparent state at $\mu=0$ for generations $n=3i-1$, being $i=1,2,\ldots$.[16] Now, for the bond problem, the elements of the transfer matrix evaluated at $\mu=0$ can be written as

$$m_{i,j}(n) = f\left(\left\lfloor\frac{x}{2}\right\rfloor + |i-j|\right)\{f(x)((-1)^{\lfloor z/5\rfloor}f(n+i-1)\gamma^{-1} - (-1)^{\lfloor y/5\rfloor}f(n+i)\gamma) - f(x+1)\}, \tag{9}$$

where $i=1,2$, $j=1,2$, $\gamma=t_B/t_A$, $f(k)=[1+(-1)^k]/2$, and the integer numbers $x=n \bmod 3 \in [0,2]$, $y=(n+2) \bmod 6 \in [0,5]$, and $z=(n+5) \bmod 6 \in [0,5]$. Therefore, the transmittance [Eq. (6)] is given by

$$\tau(\mu=0) = \frac{4}{f(x)(\gamma+\gamma^{-1})^2 + 4f(x+1)}. \tag{10}$$

Notice that the transmittance is one when $x=1$, i.e., there is a transparent state at $\mu=0$ in the bond problem for generations $n=3i+1$, being $i=1,2,\ldots$.

On the other hand, the ac conduction involves not only states at the Fermi level, but also those within an interval of $\hbar\omega$ around the Fermi energy, where ω is the angular frequency of the applied electric field. In Figs. 1(a′), 1(b′), and 1(c′), the ac conductivities at $\mu=0$ (black lines) and at $\mu=-1.88348|t|$ (gray lines) are shown for periodic, mixing and bond problems, respectively. Observe that the ac conductivity evaluated at the transparent states of periodic and mixing systems have a quite similar behavior, which is totally different from that of the bond problem, since in the latter the transparent state is located at a fractal center[17] and surrounded by nontransparent states, instead of transparent and almost transparent states in periodic and mixing cases, respectively.[10] For nontransparent states a noisy behavior is found in both mixing and bond problems. Moreover, all the dc and ac conduction spectra in Fig. 1 scale with the inverse of system size by means of $C=(N-1)[b(\gamma)]^{(3-n)/6}$, where $b(\gamma)$ is one for the periodic and mixing problems.[10] For the bond problem, $b(\gamma)$ (open circles) is plotted in Fig. 2 and compared with the scaling index $[d(\gamma)]$ of the density of states (DOS) at $\mu=0$ given by[17]

$$d(\gamma) = \frac{\ln[(\sqrt{5}+1)/2]^6}{\ln\{\sqrt{1+4[1+(\gamma-\gamma^{-1})^2/4]^2}+2[1+(\gamma-\gamma^{-1})^2/4]\}^2}. \tag{11}$$

Notice that these two scaling indexes have a similar dependence on $\gamma=t_B/t_A$, since they are tightly related through the diffusivity, as given in the Einstein relation.

In the next section, we will analyze the electronic transport in two- and three-dimensional quasiperiodic lattices.

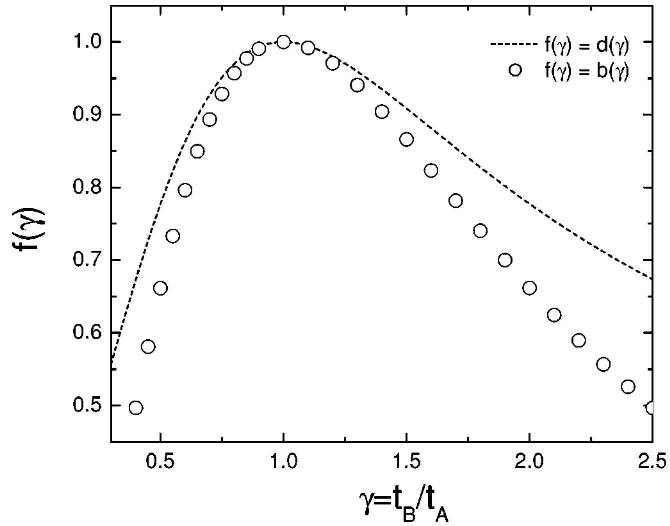

FIG. 2. The conductivity scaling factor (defined in the text) for the bond problem, $b(\gamma)$ (open circles), and the scaling index of the density of states at $\mu=0$, $d(\gamma)$ (dashed line).

III. MULTIDIMENSIONAL SYSTEMS

Let us consider a multidimensional lattice, in which one or more directions are quasiperiodic, and their Hamiltonian (H) is separable, i.e., $H=H_\parallel \otimes I_\perp + I_\parallel \otimes H_\perp$, where $H_\parallel$ $(I_\parallel)$ and $H_\perp$ $(I_\perp)$ respectively stand for the Hamiltonian (the identity of Hilbert space) of the parallel and perpendicular subsystem with respect to the applied electric field. Taking the advantage of the convolution theorem,[12] the electrical conductivity (2) of this multidimensional system can be written as (see Appendix B),

$$\sigma(\mu,\omega,T) = \frac{1}{\Omega_\perp}\int_{-\infty}^{\infty} dy\,\sigma^\parallel(\mu-y,\omega,T)\mathrm{DOS}^\perp(y), \tag{12}$$

or

$$\sigma(\mu,\omega,T) = \frac{1}{\Omega_\perp}\sum_\beta \sigma^\parallel(\mu-E_\beta,\omega,T), \tag{13}$$

where $\sigma^\parallel$ is the electrical conductivity of the parallel subsystem; $\Omega_\perp$, $\mathrm{DOS}^\perp$ and E_β are, respectively, the volume, the density of states, and the eigenvalues of the perpendicular subsystem, i.e., $H_\perp|\beta\rangle = E_\beta|\beta\rangle$. In Figs. 3(a) and 3(b), we show the dc electrical conductances at zero temperature, defined as $g(\mu,0,0)=\sigma(\mu,0,0)\ \Omega_\perp/\Omega_\parallel$, for 2D and 3D periodic lattices, respectively. Figures 3(c) and 3(d) exhibit the electrical conductances of the same systems as in Figs. 3(a) and 3(b) except that in the perpendicular directions to the applied electric field the atoms are arranged following the bond Fibonacci sequence with $\gamma=t_B/t_A=0.88$. The magnifications of Figs. 3(a)–3(d) are, respectively, illustrated in Figs. 3(a′)–3(d′). The size in each direction of these lattices is of 165580142 atoms, corresponding to the generation $n=40$, and along the electric field the system is connected to two semi-infinite periodic leads with hopping integrals t. These spectra are calculated by using Eq. (12) and the imagi-

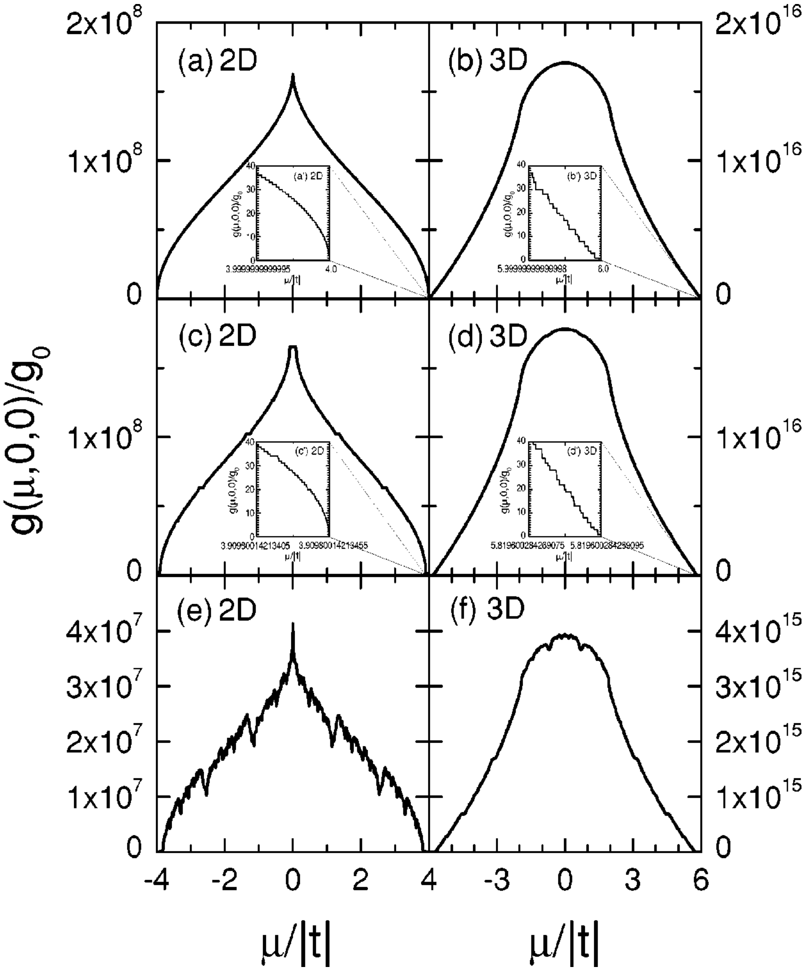

FIG. 3. The dc electrical conductances at zero temperature for (a) 2D and (b) 3D periodic lattices, (c) 2D and (d) 3D lattices with quasiperiodic order ($\gamma = t_B/t_A = 0.88$) in the perpendicular directions to the applied electric field, and (e) 2D and (f) 3D totally quasiperiodic systems, i.e. the bond Fibonacci sequence is obeyed in every direction of the systems. The magnifications of figures (a–d) are, respectively, illustrated in 3(a′)–3(d′). Each direction of these lattices has 165580142 atoms and along the electric field the system is connected to two semi-infinite periodic leads with hopping integrals t. The imaginary part (η) of the energy is $10^{-11}|t|$ for $\sigma^{\parallel}$ and $10^{-3}|t|$ for $\mathrm{DOS}^{\perp}$.

nary part (η) of the energy takes $10^{-11}|t|$ for $\sigma^{\parallel}$ and $10^{-3}|t|$ for $\mathrm{DOS}^{\perp}$. The energy mesh of these spectra has a spacing ($\Delta\mu$) of $10^{-4}|t|$ and for the insets a mesh of 10000 energies is used. Notice that for 2D periodic systems there are perfect quantum steps in units of $g_0 = 2e^2/h$, as observed in 2D electron gas devices.[18] However, in 3D periodic lattices the quantum steps are not uniform, due to the degeneracy and distribution of eigenvalues E_β in Eq. (13). For partially quasiperiodic 2D systems [see Fig. 3(c)], self-similarly distributed quantum steps are observed. In Figs. 3(e) and 3(f), we respectively show the electrical conductances of 2D and 3D totally quasiperiodic systems, i.e., the bond Fibonacci sequence is obeyed in every direction of the system. Observe that these noisy spectra are one order of magnitude smaller than those of partially quasiperiodic systems and the quantum steps are disappeared.

In order to analyze global behaviors of the spectra in figure 3, a spectral average of the conductance, defined as

$$\langle g \rangle = \frac{\int d\mu g(\mu,0,0)\mathrm{DOS}(\mu)}{\int d\mu\, \mathrm{DOS}(\mu)},$$

is investigated and it is plotted in Fig. 4(a) versus the width ($\Omega_\perp \sim N_\perp$) and in Fig. 4(b) versus the system length ($L_\parallel = N_\parallel a$) for 2D periodic lattices (open circles) and doubly quasiperiodic lattices (solid circles), with the same parameters as in Fig. 3. Observe that $\langle g \rangle$ grows linearly with $N_\perp$, that is $\langle g \rangle = g_0(\varphi N_\perp + \delta)$, where for the periodic lattices $\varphi = 0.56533$ and $\delta = 0.77847$, and for the doubly quasiperiodic lattices $\varphi = 0.12923$ and $\delta = -0.10234$. These values of δ are essentially zero if they are compared with the system width ($\sim 10^8$), and the slope (φ) is expected to be 1 for the periodic case if the parallel linear chains (or conducting channels) are totally independent. Moreover, when the system length grows, $\langle g \rangle$ is a constant for the periodic case and it decays as a power law [$\langle g \rangle = g_0 \xi N_\parallel^{-\upsilon}$] for the quasiperiodic system, as reported for finite Penrose lattices.[19] We found $\upsilon = 0.0847$ and $\xi = 103745674.8369$ for doubly quasiperiodic case. Figures 4(c) and 4(d) present the averaged conductances for three-dimensional systems, with the same parameters as 2D systems shown in Figs. 4(a) and 4(b). These conductances have a very similar behavior as 2D-system ones, except that for periodic case $\varphi = 0.44612$ and $\delta = -2.84776 \times 10^8$ and for quasiperiodic system $\varphi = 0.10324$, $\delta = 9.15914 \times 10^7$, $\upsilon = 0.08492$, and $\xi = 13747698529064202$. Again, δ is negligible in comparison with the cross section area ($\sim 10^{16}$), therefore, we obtain a general relationship as

$$\langle g \rangle = g_0 \zeta N_\perp N_\parallel^{-\upsilon},$$

where $\zeta = \xi / N_\perp = \varphi N_\parallel^{\upsilon} \simeq 0.5$.

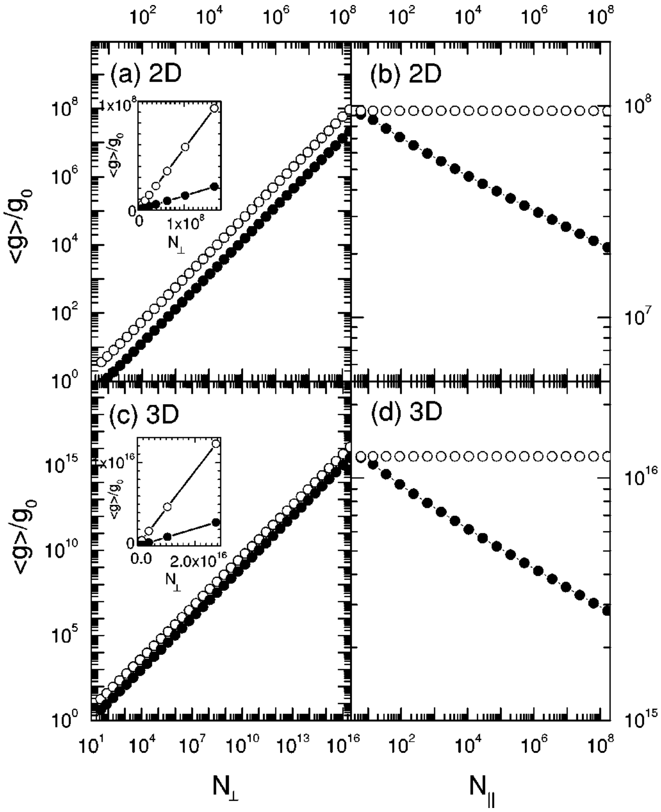

FIG. 4. Spectral average of the conductance $\langle g\rangle$ versus the width ($\Omega_\perp \sim N_\perp$) and the length ($L_\parallel = N_\parallel a$) of the system are, respectively, shown in (a) and (b) for 2D, (c) and (d) for 3D, periodic (open circles) and totally quasiperiodic lattices (solid circles), with the same parameters as in Fig. 3.

Another interesting and not widely studied feature of the dc-conductance spectrum is its dependence on the imaginary part (η) of the energy in the Green's function. In Fig. 5 we show the variation of $g(\mu,\eta)/g_0$ versus η and μ, for the same 3D system shown in Fig. 3(f). Observe that as η grows the conductance spectrum decreases keeping its shape. Figure 6 exhibits the spectral integral of the conductance

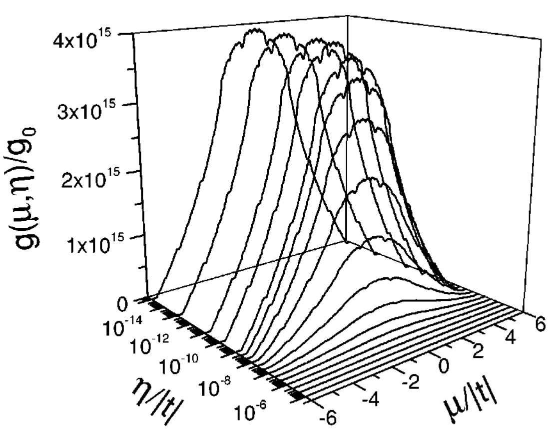

FIG. 5. The variation of dc electrical conductance at zero temperature $[g(\mu,\eta)/g_0]$ as a function of the imaginary part of the energy (η) and of the Fermi energy (μ) for a 3D totally quasiperiodic system, as shown in Fig. 3(f).

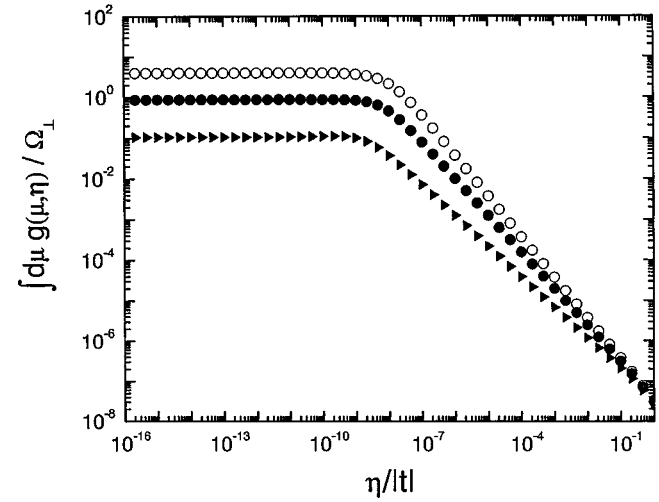

FIG. 6. The spectral integral of the conductance $[\int d\mu g(\mu,\eta)]$ as function of η for a 3D periodic lattice (open circles) and 3D bond Fibonacci lattices with $\gamma = t_B/t_A = 0.88$ (solid circles) and $\gamma = 0.75$ (solid triangles).

$[\int d\mu g(\mu,\eta)]$ in units of the perpendicular-subsystem size as a function of η for a 3D periodic lattice (open circles), and 3D bond Fibonacci lattices with $\gamma = t_B/t_A = 0.88$ (solid circles) and $\gamma = t_B/t_A = 0.75$ (solid triangles). Notice the existence of a critical value (η_c), i.e., the integrals maintain the same value for $\eta < \eta_c$ and diminish following a power law ($\eta^{-\varepsilon}$) when $\eta > \eta_c$, being $\varepsilon = 1$ for the periodic lattice, $\varepsilon = 0.90353$ and 0.7585 for bond Fibonacci systems with $\gamma = 0.88$ and 0.75, respectively. It is interesting to contrast with the DOS spectrum, whose spectral integral is always a constant, independent from η. Furthermore, we have observed that $\eta_c \sim N_\parallel^{-1}$ and for large η the integrals converge a unique value. These facts could be interpreted as the inelastic-scattering effects represented by η: when $\eta < \eta_c$ the inelastic-scattering free path is larger than the system length and then the conductance is independent of η; for $\eta > \eta_c$ the conductances of different systems reduce to the same minimum value as η increases, where the lattice-order participation is overcome by inelastic scattering effects. For 1D periodic systems, we found an analytical solution of the dc conductivity at zero temperature $[\sigma(\mu,\eta)]$ for finite values of η, as shown in Eq. (C6), and it has a simple form [Eq. (C7)] for $\mu = 0$.

IV. CONCLUSIONS

In summary, we have extended the renormalization method to the Kubo-Greenwood formula in bond Fibonacci systems. Combining with the convolution technique we are able to analyze the electronic transport in multidimensional *macroscopic* quasiperiodic systems, when their Hamiltonian is separable. It would be important to mention that this analysis has been performed in an *exact* way within the Kubo-Greenwood formalism.

For the one-dimensional case, the results of the bond problem show a qualitatively different dc and ac conductivity spectra with respect to those of mixing Fibonacci systems. We found a new kind of transparent state, which is located at a fractal center and its transfer matrices do not commute as in the mixing case.[20]

The dc electrical conductance of two- and three-dimensional Fibonacci systems show a quantized behavior when the system is periodic along the direction of the applied electric field, and these steps are redistributed in a self-similar structure when the system becomes quasiperiodic in the perpendicular direction to the electric field. The spectrally averaged conductance shows a power-law decay as the system length increases, similar to that happened in Penrose lattices. This power-law decay reveals the critical localization nature in quasiperiodic systems, contrary to the constant and exponential decay behaviors in the periodic and randomly disordered systems, respectively.[21]

The imaginary part (η) of the energy has a relevant participation in the Kubo-Greenwood formula. We find a critical value (η_c) and it is inversely proportional to the system length. For $\eta<\eta_c$ the dc conductance is independent from specific values of η and for $\eta>\eta_c$ the conductance decays with η, which can be understood if η is interpreted as the inelastic scattering strength in the system. This analysis suggests the use of $\eta<\eta_c$ for electric conductance calculations if the inelastic scattering is neglected.

Finally, this renormalization method can be extended to analyze other physical properties, such as the lattice thermal conductance[22] in quasiperiodic systems. This study is currently in progress.

ACKNOWLEDGMENTS

We gratefully acknowledge discussions with Professor D. Mayou. This work has been partially supported by CONACyT-41492F, UNAM-IN101701, and UNAM-IN122704. Computations were performed at Bakliz of DGSCA, UNAM.

APPENDIX A: RENORMALIZATION FORMULAS FOR THE BOND PROBLEM

The trace in the Kubo-Greenwood formula [Eq. (2)] for a Fibonacci chain (FC) with two kinds of bonds can be written as

$$\mathrm{Tr}[p\,\mathrm{Im}\,G^{+}(E+\hbar\omega)p\,\mathrm{Im}\,G^{+}(E)] = S(E^{+}_{\omega},E^{+},n) - S(E^{+}_{\omega},E^{-},n) - S(E^{-}_{\omega},E^{+},n) + S(E^{-}_{\omega},E^{-},n),$$

where $E^{\pm}=E\pm i\eta$, $E^{\pm}_{\omega}=E+\hbar\omega\pm i\eta$ with $\eta\to 0^{+}$, and

$$S(E^{\nu}_{\omega},E^{\kappa},n) = \sum_{j,k=1}^{N(n)-1} t_{j,j+1}t_{k,k+1}[2G_{j+1,k}(E^{\nu}_{\omega})G_{k+1,j}(E^{\kappa}) - G_{j+1,k+1}(E^{\nu}_{\omega})G_{k,j}(E^{\kappa}) - G_{j,k}(E^{\nu}_{\omega})G_{k+1,j+1}(E^{\kappa})],$$

being ν and κ either $+$ or $-$. These partial sums, $S(E^{\nu}_{\omega},E^{\kappa},n)$, may be expressed in terms of the Green's functions evaluated at the extreme sites of the FC as

$$\begin{aligned}S(E^{\nu}_{\omega},E^{\kappa},n) &= A(E^{\nu}_{\omega},E^{\kappa},n)G_{L,L}(E^{\nu}_{\omega})G_{L,L}(E^{\kappa}) \\ &+ B(E^{\nu}_{\omega},E^{\kappa},n)G_{L,R}(E^{\nu}_{\omega})G_{L,R}(E^{\kappa}) \\ &+ C(E^{\nu}_{\omega},E^{\kappa},n)G_{R,R}(E^{\nu}_{\omega})G_{R,R}(E^{\kappa}) \\ &+ D(E^{\nu}_{\omega},E^{\kappa},n)G_{L,L}(E^{\nu}_{\omega})G_{L,R}(E^{\kappa}) \\ &+ D(E^{\kappa},E^{\nu}_{\omega},n)G_{L,L}(E^{\kappa})G_{L,R}(E^{\nu}_{\omega}) \\ &+ F(E^{\nu}_{\omega},E^{\kappa},n)G_{L,L}(E^{\nu}_{\omega})G_{R,R}(E^{\kappa}) \\ &+ F(E^{\kappa},E^{\nu}_{\omega},n)G_{L,L}(E^{\kappa})G_{R,R}(E^{\nu}_{\omega}) \\ &+ I(E^{\nu}_{\omega},E^{\kappa},n)G_{L,R}(E^{\nu}_{\omega})G_{R,R}(E^{\kappa}) \\ &+ I(E^{\kappa},E^{\nu}_{\omega},n)G_{L,R}(E^{\kappa})G_{R,R}(E^{\nu}_{\omega}) \\ &+ J(E^{\nu}_{\omega},E^{\kappa},n)G_{L,L}(E^{\nu}_{\omega}) + J(E^{\kappa},E^{\nu}_{\omega},n)G_{L,L}(E^{\kappa}) \\ &+ K(E^{\nu}_{\omega},E^{\kappa},n)G_{L,R}(E^{\nu}_{\omega}) + K(E^{\kappa},E^{\nu}_{\omega},n)G_{L,R}(E^{\kappa}) \\ &+ L(E^{\nu}_{\omega},E^{\kappa},n)G_{R,R}(E^{\nu}_{\omega}) + L(E^{\kappa},E^{\nu}_{\omega},n)G_{R,R}(E^{\kappa}) \\ &+ Z(E^{\nu}_{\omega},E^{\kappa},n),\end{aligned}$$

where the subindexes L and R denote the left- and the right-end atoms, respectively. The coefficients $A(E_1,E_2,n)$, $B(E_1,E_2,n),\ldots,$ $Z(E_1,E_2,n)$ in the last equation, being E_1 and E_2 either E^{ν}_{ω} or E^{κ}, can be iteratively obtained from those of generations $n-1$ and $n-2$, as given in the following:

$$A(E_1,E_2,n) = -[A_c(E_1,E_2,n) - A_c(E_2,E_1,n)]^2,$$

$$\begin{aligned}B(E_1,E_2,n) &= 2[A_c(E_1,E_2,n) - A_c(E_2,E_1,n)][B_c(E_2,E_1,n) \\ &- B_c(E_1,E_2,n)] + 2[C_c(E_1,E_2,n) - D_c(E_2,E_1,n)] \\ &\times[C_c(E_2,E_1,n) - D_c(E_1,E_2,n)],\end{aligned}$$

$$C(E_1,E_2,n) = -[B_c(E_1,E_2,n) - B_c(E_2,E_1,n)]^2,$$

$$\begin{aligned}D(E_1,E_2,n) &= 2[A_c(E_1,E_2,n) - A_c(E_2,E_1,n)][D_c(E_2,E_1,n) \\ &- C_c(E_1,E_2,n)],\end{aligned}$$

$$F(E_1,E_2,n) = -[C_c(E_1,E_2,n) - D_c(E_2,E_1,n)]^2,$$

$$\begin{aligned}I(E_1,E_2,n) &= 2[B_c(E_1,E_2,n) - B_c(E_2,E_1,n)][D_c(E_2,E_1,n) \\ &- C_c(E_1,E_2,n)],\end{aligned}$$

$$\begin{aligned}J(E_1,E_2,n) &= J(E_1,E_2,n-1) + \theta_0(E_2,n)F(E_1,E_2,n-1) \\ &+ \theta_1(E_1,n)K(E_1,E_2,n-1) + \theta_1^2(E_1,n)\theta_0(E_2,n) \\ &\times[C(E_1,E_2,n-1) + A(E_1,E_2,n-2) \\ &+ A_o(E_1,E_2,n)] + \theta_0(E_2,n)\theta_1(E_1,n) \\ &\times[I(E_1,E_2,n-1) + B_o(E_1,E_2,n)] + \theta_1^2(E_1,n) \\ &\times[L(E_1,E_2,n-1) + J(E_1,E_2,n-2)],\end{aligned}$$

$$K(E_1,E_2,n) = 2\theta_0(E_2,n)\theta_1(E_1,n)\theta_2(E_1,n)[C(E_1,E_2,n-1) + A(E_1,E_2,n-2) + A_o(E_1,E_2,n)] + \theta_0(E_2,n)C_o(E_1,E_2,n) + 2\theta_1(E_1,n)\theta_2(E_1,n) \times[L(E_1,E_2,n-1) + J(E_1,E_2,n-2)] + \theta_0(E_2,n) \times\{\theta_1(E_1,n)[D(E_2,E_1,n-2) + D_o(E_2,E_1,n)] + \theta_2(E_1,n)[I(E_1,E_2,n-1) + B_o(E_1,E_2,n)]\} + \theta_2(E_1,n)K(E_1,E_2,n-1) + \theta_1(E_1,n)K(E_1,E_2,n-2),$$

$$L(E_1,E_2,n) = L(E_1,E_2,n-2) + \theta_0(E_2,n)F(E_2,E_1,n-2) + \theta_2(E_1,n)K(E_1,E_2,n-2) + \theta_2^2(E_1,n)\theta_0(E_2,n) \times[C(E_1,E_2,n-1) + A(E_1,E_2,n-2) + A_o(E_1,E_2,n)] + \theta_0(E_2,n)\theta_2(E_1,n)[D(E_2,E_1,n-2) + D_o(E_2,E_1,n)] + \theta_2^2(E_1,n)[L(E_1,E_2,n-1) + J(E_1,E_2,n-2)],$$

$$Z(E_1,E_2,n) = \theta_0(E_1,n)[L(E_1,E_2,n-1) + J(E_1,E_2,n-2)] + Z(E_1,E_2,n-1) + \theta_0(E_1,n)\theta_0(E_2,n) \times[C(E_1,E_2,n-1) + A(E_1,E_2,n-2) + A_o(E_1,E_2,n)] + \theta_0(E_2,n)[L(E_2,E_1,n-1) + J(E_2,E_1,n-2)] + Z(E_1,E_2,n-2),$$

where

$$\theta_0(E,n) = [E - E_R(E,n-1) - E_L(E,n-2)]^{-1},$$

$$\theta_1(E,n) = t(E,n-1)\theta_0(E,n),\quad \theta_2(E,n) = t(E,n-2)\theta_0(E,n),$$

$$A_c(E_1,E_2,n) = A_c(E_1,E_2,n-1) + \theta_1(E_1,n)\theta_1(E_2,n) \times[A_c(E_1,E_2,n-2) + B_c(E_1,E_2,n-1)] + \theta_1(E_2,n)C_c(E_1,E_2,n-1) + \theta_1(E_1,n)D_c(E_1,E_2,n-1),$$

$$B_c(E_1,E_2,n) = B_c(E_1,E_2,n-2) + \theta_2(E_1,n)\theta_2(E_2,n) \times[A_c(E_1,E_2,n-2) + B_c(E_1,E_2,n-1)] + \theta_2(E_1,n)C_c(E_1,E_2,n-2) + \theta_2(E_2,n)D_c(E_1,E_2,n-2),$$

$$C_c(E_1,E_2,n) = \theta_1(E_1,n)\theta_2(E_2,n)[A_c(E_1,E_2,n-2) + B_c(E_1,E_2,n-1)] + \theta_2(E_2,n)C_c(E_1,E_2,n-1) + \theta_1(E_1,n)C_c(E_1,E_2,n-2),$$

$$D_c(E_1,E_2,n) = \theta_1(E_2,n)\theta_2(E_1,n)[A_c(E_1,E_2,n-2) + B_c(E_1,E_2,n-1)] + \theta_2(E_1,n)D_c(E_1,E_2,n-1) + \theta_1(E_2,n)D_c(E_1,E_2,n-2),$$

$$A_o(E_1,E_2,n) = 2[A_c(E_1,E_2,n-2) - A_c(E_2,E_1,n-2)] \times[B_c(E_2,E_1,n-1) - B_c(E_1,E_2,n-1)],$$

$$B_o(E_1,E_2,n) = 2[A_c(E_1,E_2,n-2) - A_c(E_2,E_1,n-2)] \times[D_c(E_2,E_1,n-1) - C_c(E_1,E_2,n-1)],$$

$$C_o(E_1,E_2,n) = 2[D_c(E_1,E_2,n-2) - C_c(E_2,E_1,n-2)] \times[D_c(E_2,E_1,n-1) - C_c(E_1,E_2,n-1)],$$

$$D_o(E_1,E_2,n) = 2[B_c(E_1,E_2,n-1) - B_c(E_2,E_1,n-1)] \times[D_c(E_2,E_1,n-2) - C_c(E_1,E_2,n-2)],$$

being E either E_1 or E_2. The effective hopping integral, $t(E,n)$, and the effective self-energies of the left and right extreme sites, $E_L(E,n)$ and $E_R(E,n)$, are given by

$$t(E,n) = t(E,n-1)t(E,n-2)\theta_0(E,n),$$

$$E_L(E,n) = E_L(E,n-1) + t^2(E,n-1)\theta_0(E,n),$$

$$E_R(E,n) = E_R(E,n-2) + t^2(E,n-2)\theta_0(E,n).$$

For the case of free boundary conditions, the Green's functions at the ends of the system are

$$G_{L,L}(E) = [E - E_R(E,n)]/\gamma_G,$$

$$G_{R,R}(E) = [E - E_L(E,n)]/\gamma_G,$$

$$G_{L,R}(E) = t(E,n)/\gamma_G,$$

where $\gamma_G=[E-E_L(E,n)]\,[E-E_R(E,n)]-t^2(E,n)$, and for the case of finite-lead boundary conditions, they are

$$G_{L,L}(E) = \left\{E - E_L(E,n) - E_{RP}(E,m) - \frac{t_P^2(E,m)}{E - E_{LP}(E,m)} - \frac{t^2(E,n)}{E - E_R(E,n) - E_{LP}(E,m) - t_P^2(E,m)/[E - E_{RP}(E,m)]}\right\}^{-1},$$

$$G_{R,R}(E) = \left\{E - E_R(E,n) - E_{LP}(E,m) - \frac{t_P^2(E,m)}{E - E_{RP}(E,m)} - \frac{t^2(E,n)}{E - E_L(E,n) - E_{RP}(E,m) - t_P^2(E,m)/[E - E_{LP}(E,m)]}\right\}^{-1},$$

$$G_{L,R}(E) = \frac{G_{R,R}(E)t(E,n)}{\{E - E_L(E,n) - E_{RP}(E,m) - t_P^2(E,m)/[E - E_{LP}(E,m)]\}},$$

where m is the generation number of the *periodic* leads built following the Fibonacci procedure, and their effective self-energies and effective hopping are given by

$$E_{LP}(E,m) = E_{LP}(E,m-1) + t_P^2(E,m-1)/\gamma_P(E,m),$$

$$E_{RP}(E,m) = E_{RP}(E,m-2) + t_P^2(E,m-2)/\gamma_P(E,m),$$

$$t_P(E,m) = t_P(E,m-1)t_P(E,m-2)/\gamma_P(E,m),$$

being

$$\gamma_P(E,m) = [E - E_{RP}(E,m-1) - E_{LP}(E,m-2)].$$

Finally, the initial conditions for the iterative procedure are

$$t(E,1) = t_A,\ E_L(E,1) = E_R(E,1) = 0,\ t_P(E,1) = t,\quad E_{RP}(E,1) = E_{LP}(E,1) = 0,$$

$$t(E,2) = t_A t_B/E,\ E_L(E,2) = t_B^2/E,\ E_R(E,2) = t_A^2/E,$$

$$t_P(E,2) = t^2/E,\ E_{LP}(E,2) = E_{RP}(E,2) = t_P(E,2),$$

$$A(E_1,E_2,1) = C(E_1,E_2,1) = D(E_1,E_2,1) = I(E_1,E_2,1) = 0,\ B(E_1,E_2,1) = 2t_A^2,$$

$$J(E_1,E_2,1) = K(E_1,E_2,1) = L(E_1,E_2,1) = Z(E_1,E_2,1) = 0,\ F(E_1,E_2,1) = -t_A^2,$$

$$A(E_1,E_2,2) = -[t(E_1,2) - t(E_2,2)]^2 t_B^2/t_A^2,\ B(E_1,E_2,2) = 4[t^2(E_1,2) + t^2(E_2,2)],$$

$$C(E_1,E_2,2) = -[t(E_1,2) - t(E_2,2)]^2 t_A^2/t_B^2,\quad D(E_1,E_2,2) = 2[t^2(E_1,2) - t^2(E_2,2)]t_B/t_A,$$

$$F(E_1,E_2,2) = -[t(E_1,2) + t(E_2,2)]^2,\quad I(E_1,E_2,2) = 2[t^2(E_2,2) - t^2(E_1,2)]t_A/t_B,$$

$$J(E_1,E_2,2) = -t(E_2,2)t_B/t_A,\ K(E_1,E_2,2) = 2t(E_2,2),$$

$$L(E_1,E_2,2) = -t(E_2,2)t_A/t_B,\ Z(E_1,E_2,2) = 0,$$

$$A_c(E_1,E_2,1) = B_c(E_1,E_2,1) = C_c(E_1,E_2,1) = 0,\quad D_c(E_1,E_2,1) = t_A,$$

$$A_c(E_1,E_2,2) = t_B^2/E_1,\ B_c(E_1,E_2,2) = t_A^2/E_2,$$

$$C_c(E_1,E_2,2) = 0,\ D_c(E_1,E_2,2) = t_A t_B/E_1 + t_A t_B/E_2.$$

For the case of the density of states (DOS), the renormalization procedure is much simpler, since only a sum of diagonal elements of Green's functions is involved, instead of products of them in the Kubo-Greenwood formula. In this case, we have

$$\begin{aligned}\mathrm{DOS}(E) &= -\frac{1}{\pi}\,\mathrm{Im}\sum_j G_{j,j}(E^+)\\ &= -\frac{1}{\pi}\,\mathrm{Im}\{D_1(E^+,n)G_{L,L}(E^+) + D_2(E^+,n)G_{R,R}(E^+)\\ &\quad + D_3(E^+,n)G_{L,R}(E^+) + D_4(E^+,n)\},\end{aligned} \tag{A1}$$

where

$$\begin{aligned}D_1(E^+,N) &= D_1(E^+,N-1) + \theta_1^2(E^+,n)[D_1(E^+,N-2) + D_2(E^+,N-1) - 1] + \theta_1(E^+,n)D_3(E^+,N-1),\\
D_2(E^+,N) &= D_2(E^+,N-2) + \theta_2^2(E^+,n)[D_2(E^+,N-1) + D_1(E^+,N-2) - 1] + \theta_2(E^+,n)D_3(E^+,N-2),\\
D_3(E^+,N) &= \theta_2(E^+,n)D_3(E^+,N-1) + \theta_1(E^+,n)D_3(E^+,N-2) + 2\theta_2(E^+,n)\theta_1(E^+,n)\\ &\quad\times[D_1(E^+,N-2) + D_2(E^+,N-1) - 1],\\
D_4(E^+,N) &= D_4(E^+,N-1) + D_4(E^+,N-2) + \theta_0(E^+,n)\\ &\quad\times[D_1(E^+,N-2) + D_2(E^+,N-1) - 1],\end{aligned}$$

and the initial conditions are

$$D_1(E^+,1) = D_2(E^+,1) = 1,\ D_3(E^+,1) = D_4(E^+,1) = 0,$$

$$D_1(E^+,2) = 1 + \frac{t_B^2}{(E^+)^2},\ D_2(E^+,2) = 1 + \frac{t_A^2}{(E^+)^2},$$

$$D_3(E^+,2) = \frac{2t_B t_A}{(E^+)^2},\ D_4(E^+,2) = \frac{1}{E^+}.$$

This renormalization method is very efficient, as discussed in Section II, and it is recommended to use *quadruple* precision for the numerical evaluations.

APPENDIX B: CONVOLUTION FORMULA

For a given Hamiltonian H, the corresponding Green's function (G) can be expressed as

$$G_{lk}(z)=\sum_{\alpha}\frac{\langle l|\alpha\rangle\langle\alpha|k\rangle}{z-E_{\alpha}},\qquad\text{(B1)}$$

where $z=E+i\eta$ is a complex number, the eigenstates ($|\alpha>$) are determined by $H|\alpha\rangle=E_{\alpha}|\alpha\rangle$, $|l\rangle$ and $|k\rangle$ are Wannier's functions of sites l and k, respectively. Equation (B1) can be rewritten as

$$-\frac{1}{\pi}\,\mathrm{Im}[G_{lk}(z)]=\sum_{\alpha}\langle l|\alpha\rangle\langle\alpha|k\rangle\delta(E-E_{\alpha}),\qquad\text{(B2)}$$

since

$$\lim_{\eta\to 0}\frac{1}{x\pm i\eta}=P\left(\frac{1}{x}\right)\mp i\pi\delta(x).$$

If H is separable, i.e., $H=H_{\parallel}\otimes I_{\perp}+I_{\parallel}\otimes H_{\perp}$, its eigenvalues and eigenfunctions can be respectively written as $E=E_{\alpha}+E_{\beta}$ and $|\alpha,\beta\rangle=|\alpha\rangle|\beta\rangle$, where $H_{\parallel}|\alpha\rangle=E_{\alpha}|\alpha\rangle$, $H_{\perp}|\beta\rangle=E_{\beta}|\beta\rangle$, $I_{\perp}$ and $I_{\parallel}$ respectively stand for the identities of the perpendicular and parallel subsystem with respect to the applied electric field. Thus, the Green's function is given by

$$G_{(r,j)(k,l)}(z)=\sum_{\alpha,\beta}\frac{\langle r|\alpha\rangle\langle\alpha|k\rangle\langle j|\beta\rangle\langle\beta|l\rangle}{z-(E_{\alpha}+E_{\beta})},$$

where r and k are site coordinates in the parallel subspace, while j and l are site coordinates in the perpendicular subspace. Moreover, using Eq. (B2) we have

$$\begin{aligned}G_{(r,j)(k,l)}(z+\hbar\omega)&=\int_{-\infty}^{\infty}dy\sum_{\alpha,\beta}\frac{\langle r|\alpha\rangle\langle\alpha|k\rangle\langle j|\beta\rangle\langle\beta|l\rangle}{z+\hbar\omega-(E_{\alpha}+y)}\delta(y-E_{\beta})\\&=-\frac{1}{\pi}\lim_{\eta'\to 0}\int_{-\infty}^{\infty}dy\sum_{\alpha}\frac{\langle r|\alpha\rangle\langle\alpha|k\rangle}{z+\hbar\omega-(E_{\alpha}+y)}\\&\quad\times\mathrm{Im}[G_{jl}^{\perp}(y+i\eta')]\\&=-\frac{1}{\pi}\lim_{\eta'\to 0}\int_{-\infty}^{\infty}dy\,G_{rk}^{\parallel}(z+\hbar\omega-y)\\&\quad\times\mathrm{Im}[G_{jl}^{\perp}(y+i\eta')].\end{aligned}\qquad\text{(B3)}$$

In the Kubo-Greenwood formula [Eq. (2)], the projection of the momentum operator (p) is along of the applied electric field, i.e., $p_{(k,l)(f,s)}=p_{kf}^{\parallel}\delta_{l,s}$ is in the parallel subspace. Using Eq. (B3) and (B2) one obtains

$$\begin{aligned}\mathrm{Tr}[p\,\mathrm{Im}\,G^{+}(z+\hbar\omega)p\,\mathrm{Im}\,G^{+}(z)]&=\sum_{r,j,k,l,f,s,v,w}\{p_{(v,w)(r,j)}\,\mathrm{Im}[G_{(r,j)(k,l)}(z+\hbar\omega)]p_{(k,l)(f,s)}\,\mathrm{Im}[G_{(f,s)(v,w)}(z)]\}\\&=\sum_{r,j,k,l,f,v}\{p_{vr}^{\parallel}\,\mathrm{Im}[G_{(r,j)(k,l)}(z+\hbar\omega)]p_{kf}^{\parallel}\,\mathrm{Im}[G_{(f,l)(v,j)}(z)]\}\\&=\frac{1}{\pi^{2}}\sum_{r,j,k,l,f,v}p_{vr}^{\parallel}\int_{-\infty}^{\infty}dx\,\mathrm{Im}[G_{rk}^{\parallel}(z+\hbar\omega-x)]\mathrm{Im}[G_{jl}^{\perp}(x+i\eta')]\\&\quad\times p_{kf}^{\parallel}\int_{-\infty}^{\infty}dy\,\mathrm{Im}[G_{fv}^{\parallel}(z-y)]\mathrm{Im}[G_{lj}^{\perp}(y+i\eta'')]\\&=\sum_{r,j,k,l,f,v}\int_{-\infty}^{\infty}dx\int_{-\infty}^{\infty}dy\,p_{vr}^{\parallel}\,\mathrm{Im}[G_{rk}^{\parallel}(z+\hbar\omega-x)]p_{kf}^{\parallel}\,\mathrm{Im}[G_{fv}^{\parallel}(z-y)]\\&\quad\times\left[\sum_{\beta'}\langle j|\beta'\rangle\langle\beta'|l\rangle\delta(x-E_{\beta'})\right]\left[\sum_{\beta}\langle l|\beta\rangle\langle\beta|j\rangle\delta(y-E_{\beta})\right]\\&=\sum_{r,k,f,v}\int_{-\infty}^{\infty}dy\,p_{vr}^{\parallel}\,\mathrm{Im}[G_{rk}^{\parallel}(z+\hbar\omega-y)]p_{kf}^{\parallel}\,\mathrm{Im}[G_{fv}^{\parallel}(z-y)]\times\left[\sum_{\beta}\delta(y-E_{\beta})\right].\end{aligned}\qquad\text{(B4)}$$

Therefore, considering $\mathrm{DOS}^{\perp}(y)=\Sigma_{\beta}\delta(y-E_{\beta})$, we obtain the well known convolution relationship[12]

$$\sigma(E,\omega,T)=\frac{1}{\Omega_{\perp}}\int_{-\infty}^{\infty}dy\,\sigma^{\parallel}(E-y,\omega,T)\mathrm{DOS}^{\perp}(y),\qquad\text{(B5)}$$

where

$$\sigma^{\|}(E,\omega,T) = \lim_{\eta\to 0^+} \frac{2e^2\hbar}{\pi\Omega_{\|}m^2}\int_{-\infty}^{\infty} dE \frac{f(E)-f(E+\hbar\omega)}{\hbar\omega} \times \sum_{r,k,f,v} p^{\|}_{vr}\,\mathrm{Im}[G^{\|}_{rk}(z+\hbar\omega)]p^{\|}_{kf}\,\mathrm{Im}[G^{\|}_{fv}(z)].$$

Finally, Eq. (B4) can also be written as

$$\sigma(E,\omega,T) = \frac{1}{\Omega_\perp}\sum_\beta \sigma^{\|}(E-E_\beta,\omega,T). \tag{B6}$$

This last formulation could particularly be useful for systems with a small cross section perpendicular to the applied electric field, such as quantum wires and nanotubes.

APPENDIX C: KUBO CONDUCTIVITY OF PERIODIC CHAINS

In this appendix we present an analytical solution of the Kubo-Greenwood formula for a periodic chain of N atoms, with lattice constant a, null self-energies and hopping integrals t, saturated by two semi-infinite periodic chains with the same parameters. The linear momentum operator for this case is given by

$$p = \frac{imat}{\hbar}\sum_j \{|j\rangle\langle j+1| - |j\rangle\langle j-1|\},$$

and then the trace in the Kubo-Greenwood formula [Eq. (2)] can be written as

$$\begin{aligned}
&\mathrm{Tr}[p\,\mathrm{Im}\,G^+(E+\hbar\omega)p\,\mathrm{Im}\,G^+(E)] \\
&= -\left(\frac{mat}{\hbar}\right)^2 \sum_{j,k=1}^{N(n)-1} [\mathrm{Im}\,G_{j+1,k}(E^+_\omega)\mathrm{Im}\,G_{k+1,j}(E^+) \\
&\quad + \mathrm{Im}\,G_{j+1,k}(E^+)\mathrm{Im}\,G_{k+1,j}(E^+_\omega) \\
&\quad - \mathrm{Im}\,G_{j+1,k+1}(E^+_\omega)\mathrm{Im}\,G_{k,j}(E^+) \\
&\quad - \mathrm{Im}\,G_{j,k}(E^+_\omega)\mathrm{Im}\,G_{k+1,j+1}(E^+)],
\end{aligned} \tag{C1}$$

being $E^+=E+i\eta$, $E_\omega=E+\hbar\omega$, and then $E^+_\omega=E+\hbar\omega+i\eta$ with $\eta\to 0^+$. For a periodic chain, the Green's function is given by[23]

$$G_{j,k}(E^+_l) = \frac{\left[\left(E^+_l - \sqrt{(E^+_l)^2-(2t)^2}\right)/(2|t|)\right]^{|j-k|}}{\sqrt{(E^+_l)^2-(2t)^2}},$$

where $E^+_l=E_l+i\eta$, $E_l=E$ or E_ω, and the imaginary part of $\sqrt{(E^+_l)^2-(2t)^2}$ should have the same sign as $\mathrm{Im}\{E^+_l\}=\eta$. Now, let us define

$$\cos\phi_l = \frac{E_l^2-\eta^2-(2t)^2}{A_l},\ \sin\phi_l = \frac{2|E_l|\eta}{A_l},$$

$$\cos\theta_l = \frac{|E_l|-\sqrt{A_l}\cos(\phi_l/2)}{2|t|B_l},\ \text{and}\ \sin\theta_l = \frac{\eta-\sqrt{A_l}\sin(\phi_l/2)}{2|t|B_l},$$

where

$$A_l = \sqrt{(E_l^2-\eta^2-4t^2)^2+4\eta^2E_l^2},$$

and

$$B_l = \sqrt{\left[\frac{|E_l|-\sqrt{A_l}\cos(\phi_l/2)}{2t}\right]^2+\left[\frac{\eta-\sqrt{A_l}\sin(\phi_l/2)}{2t}\right]^2}.$$

Hence

$$G_{j,k}(E^+_l) = \frac{B_l^{|j-k|}}{\sqrt{A_l}}\exp[i(|j-k|\theta_l-\phi_l/2)]. \tag{C2}$$

Substituting Eq. (C2) in Eq. (C1) and taking advantage of the dumb indexes, we obtain

$$\begin{aligned}
\mathrm{Tr}[p\,\mathrm{Im}\,G^+(E+\hbar\omega)p\,\mathrm{Im}\,G^+(E)] &= -\left(\frac{mat}{\hbar}\right)^2\frac{2}{\sqrt{A_\omega A}}\sum_{j,k=1}^{N(n)-1}\{B_\omega^{|j+1-k|}B^{|k+1-j|}\sin(|j+1-k|\theta_\omega-\phi_\omega/2)\sin(|k+1-j|\theta-\phi/2) \\
&\quad - B_\omega^{|j-k|}B^{|k-j|}\sin(|j-k|\theta_\omega-\phi_\omega/2)\sin(|k-j|\theta-\phi/2)\} \\
&= -\left(\frac{mat}{\hbar}\right)^2\frac{2}{\sqrt{A_\omega A}}\Big\{(N-1)[B_\omega B\sin(\theta_\omega-\phi_\omega/2)\sin(\theta-\phi/2)-\sin(\phi_\omega/2)\sin(\phi/2)] \\
&\quad - 2\sum_{m=1}^{N(n)-2}(B_\omega B)^m(N-1-m)\sin[m\theta_\omega-\phi_\omega/2]\sin[m\theta-\phi/2] \\
&\quad + \sum_{m=1}^{N(n)-2}B_\omega^{m+1}B^{m-1}(N-1-m)\sin[(m+1)\theta_\omega-\phi_\omega/2]\sin[(m-1)\theta-\phi/2]
\end{aligned}$$

$$+\sum_{m=1}^{N(n)-2} B_{\omega}^{m-1}B^{m+1}(N-1-m)\sin[(m-1)\theta_{\omega}-\phi_{\omega}/2]\sin[(m+1)\theta-\phi/2]\Bigg\}. \tag{C3}$$

Using the following relations:

$$\sin(x)=\frac{e^{ix}-e^{-ix}}{2i},$$

$$\sum_{j=1}^{N(n)-2}(N-1-j)\cos(j\alpha_l-\gamma_l)=\mathrm{Re}\left\{\sum_{j=1}^{N(n)-2}(N-1-j)\exp[i(j\alpha_l-\gamma_l)]\right\},$$

$$\sum_{j=1}^{N(n)-2}(N-1)\exp[i(j\alpha_l-\gamma_l)]=(N-1)\exp(-i\gamma_l)\left[\frac{1-\exp[i(N-1)\alpha_l]}{1-\exp(i\alpha_l)}-1\right],$$

and

$$\sum_{j=1}^{N(n)-2} j\exp[i(j\alpha_l-\gamma_l)]=\exp(-i\gamma_l)\frac{-(N-1)\exp[i(N-1)\alpha_l]+(N-2)\exp(iN\alpha_l)+\exp(i\alpha_l)}{[1-\exp(i\alpha_l)]^2}.$$

Then, Eq. (C3) is reduced to

$$\begin{aligned}\mathrm{Tr}[p\,\mathrm{Im}\,G^{+}(E+\hbar\omega)p\,\mathrm{Im}\,G^{+}(E)]=-\frac{2(mat)^2}{\hbar^2\sqrt{A_{\omega}A}}\Bigg\{&(N-1)[B_{\omega}B\sin(\theta_{\omega}-\phi_{\omega}/2)\sin(\theta-\phi/2)-\sin(\phi_{\omega}/2)\sin(\phi/2)]\\&+\mathrm{Re}\Bigg\{\frac{\exp[i(\alpha_1-\gamma_1)][B_{\omega}B-(B_{\omega}^2/2)\exp(i\alpha_2)-(B^2/2)\exp(-i\alpha_2)]}{[1-B_{\omega}B\exp(i\alpha_1)]^2}\\&\times[(N-2)-(N-1)B_{\omega}B\exp(i\alpha_1)+(B_{\omega}B)^{N-1}\exp[i(N-1)\alpha_1]]\Bigg\}\\&-\mathrm{Re}\Bigg\{\frac{\exp[i(\alpha_2-\gamma_2)][B_{\omega}B-(B_{\omega}^2/2)\exp(i\alpha_1)-(B^2/2)\exp(-i\alpha_1)]}{[1-B_{\omega}B\exp(i\alpha_2)]^2}\\&\times[(N-2)-(N-1)B_{\omega}B\exp(i\alpha_2)+(B_{\omega}B)^{N-1}\exp[i(N-1)\alpha_2]]\Bigg\}\Bigg\},\end{aligned} \tag{C4}$$

where $\alpha_1=\theta_{\omega}+\theta$, $\alpha_2=\theta_{\omega}-\theta$, $\gamma_1=(\phi_{\omega}+\phi)/2$, and $\gamma_2=(\phi_{\omega}-\phi)/2$.

In the limit of $\eta\to 0^{+}$, we have $B=B_{\omega}=\sin(\phi/2)=\sin(\phi_{\omega}/2)=1$ and $\cos(\phi/2)=\cos(\phi_{\omega}/2)=0$. Defining $V(N)=1-\cos(N\theta)\cos(N\theta_{\omega})$ and $S(N)=\sin(N\theta)\sin(N\theta_{\omega})$, and using Eq. (C4), Eq. (2) can written as

$$\sigma(\mu,\omega,T)=\frac{8e^2t^2a}{\pi(N-1)\hbar^3\omega^2}\int_{-\infty}^{\infty}dE\frac{f(E)-f(E+\hbar\omega)}{\hbar\omega}\left\{\frac{1}{2}V(N-1)\left(\frac{V^2(1)}{S(1)}+S(1)\right)-S(N-1)V(1)\right\},$$

as obtained in Ref. 13. Furthermore, when $T\to 0$, we have $f(E)-f(E+\hbar\omega)=\theta(E-\mu)-\theta(E+\hbar\omega-\mu)$, hence

$$\begin{aligned}\sigma(\mu,\omega,0)&=\frac{8e^2t^2a}{\pi(N-1)\hbar^4\omega^3}\int_{\mu-\hbar\omega}^{\mu}dE\left\{\frac{1}{2}V(N-1)\left(\frac{V^2(1)}{S(1)}+S(1)\right)-S(N-1)V(1)\right\}\\&=\frac{8e^2t^2a}{\pi(N-1)\hbar^3\omega^2}\left[1-\left(\frac{\mu}{2t}\right)^2\right]\left\{1-\cos\left[(N-1)\frac{\hbar\omega/(2t)}{\sqrt{1-[\mu/(2t)]^2}}\right]\right\}.\end{aligned} \tag{C5}$$

On the other hand, using Eq. (C4) and in the limits of $\omega\to 0$ and $T\to 0$, Eq. (2) for finite η can be written as

$$\sigma(\mu,0,0) = -\frac{4e^2a^2t^2}{\pi\Omega\hbar A}\left\{(N-1)[B^2\sin^2(\theta-\phi/2)-\sin^2(\phi/2)] - 2\sin^2(\theta)\left[\frac{(B^2)^N-(N-1)(B^2)^2+(N-2)B^2}{(1-B^2)^2}\right]\right\}$$
$$= -\frac{4e^2a^2t^2}{\pi\Omega\hbar A}\left\{\frac{(N-1)[A(\eta^2+\mu^2-4t^2)-8t^2(2t^2+\eta^2-\mu^2)-(\eta^2+\mu^2)^2]}{8t^2A} - \frac{[\eta-\sqrt{(A-\mu^2+\eta^2+4t^2)/2}]^2[(B^2)^{N-1}-(N-1)(B^2)+(N-2)]}{2t^2(1-B^2)^2}\right\}, \tag{C6}$$

and in the limit $\mu\to 0$,

$$\sigma(0,0,0) = \frac{e^2a}{\pi\hbar[1+(\eta/2t)^2]}\left\{\sqrt{1+\left(\frac{2t}{\eta}\right)^2} + \frac{2t^2}{\eta^2(N-1)}\left[\left(\frac{\eta-\sqrt{\eta^2+4t^2}}{2t}\right)^{2N-2} - 1\right]\right\}. \tag{C7}$$

This formula reveals the existence of a critical value of $\eta(\eta_c)$, where $\eta_c \sim |t|/N$. For $\eta < \eta_c$, σ is essentially a constant and it decays following a power law for $\eta > \eta_c$.

---

[1] F. Piéchon, Phys. Rev. Lett. **76**, 4372 (1996).
[2] Z.M. Stadnik, *Physical Properties of Quasicrystals* (Springer-Verlag, Berlin Heidelberg, 1999).
[3] C.C. Homes, T. Timusk, X. Wu, Z. Altounian, A. Sahnoune, and J.O. Ström-Olsen, Phys. Rev. Lett. **67**, 2694 (1991).
[4] A. Sütö, in *Beyond Quasicrystals*, edited by F. Axel and D. Gratias (Les Editions de Physique, France, 1994), p. 483.
[5] M. Kohmoto, L.P. Kadanoff, and C. Tang, Phys. Rev. Lett. **50**, 1870 (1983).
[6] Q. Niu and F. Nori, Phys. Rev. Lett. **57**, 2057 (1986).
[7] J.A. Ashraff and R.B. Stinchcombe, Phys. Rev. B **37**, 5723 (1988).
[8] R.A. Barrio and C. Wang, in *Quasicrystal and Incommensurate Structures in Condensed Matter*, edited by M. José-Yacaman, D. Romeu, V. Castaño, and A. Gömez (World Scientific, Singapore, 1990), p. 448.
[9] A. Ghosh and S.N. Karmakar, Phys. Rev. B **57**, 2834 (1998).
[10] V. Sánchez, L.A. Pérez, R. Oviedo-Roa, and C. Wang, Phys. Rev. B **64**, 174205 (2001).
[11] G.G. Naumis, R.A. Barrio, and C. Wang, Phys. Rev. B **50**, 9834 (1994).
[12] W.A. Schwalm and M.K. Schwalm, Phys. Rev. B **37**, 9524 (1988).
[13] R. Oviedo-Roa, L.A. Pérez, and C. Wang, Phys. Rev. B **62**, 13 805 (2000).
[14] B. Kramer and A. MacKinon, Rep. Prog. Phys. **56**, 1469 (1993).
[15] Y. Imry and R. Landauer, Rev. Mod. Phys. **71**, S306 (1999).
[16] X. Huang and C. Gong, Phys. Rev. B **58**, 739 (1998).
[17] M. Kohmoto, B. Sutherland, and C. Tang, Phys. Rev. B **35**, 1020 (1987).
[18] R. de Picciotto, H.L. Stormer, L.N. Pfeiffer, K.W. Baldwin, and K.W. West, Nature (London) **411**, 51 (2001).
[19] H. Tsunetsugu, and K. Ueda, Phys. Rev. B **43**, 8892 (1991).
[20] E. Maciá and F. Domínguez-Adame, Phys. Rev. Lett. **76**, 2957 (1996).
[21] A. García-Martín and J.J. Sáenz, Phys. Rev. Lett. **87**, 116603 (2001).
[22] J.K. Flicker and P.L. Leath, Phys. Rev. B **7**, 2296 (1973).
[23] E.N. Economou, *Green's Functions in Quantum Physics* (Springer-Verlag, New York, 1983), p. 80.